

Infrared spectroscopic demonstration of a conformational change in bacteriorhodopsin involved in proton pumping

(conformational relaxation)

PÁL ORMOS

Department of Physics, University of Illinois, 1110 West Green Street, Urbana, IL 61801; and Institute of Biophysics, Biological Research Center of the Hungarian Academy of Sciences, Szeged, Odesszai krt 62, Hungary

Communicated by Hans Frauenfelder, September 27, 1990 (received for review July 17, 1990)

ABSTRACT Infrared spectral changes in bacteriorhodopsin (bR) were followed during the slow decay of the M intermediate in the temperature region 240–260 K. The decay of the M form is characterized by the disappearance of the ethylenic bands and the bands indicating the reprotonation of the Schiff base. The route of Schiff-base reprotonation completely changes between 240 K and 260 K. At 240 K reprotonation occurs from Asp-85, the group to which the proton was released during M formation, and there is no pumping. At 260 K Schiff-base reprotonation takes place through Asp-96 from the cytoplasmic side, in the normal sequence assumed for proton pumping. The dramatic change in the route of Schiff-base reprotonation is coupled to a protein conformational change characterized by the change of the ratio of the two amide I bands at 1658 cm^{-1} and 1669 cm^{-1} . This conformational change is interpreted as the conformational switch crucial for proton pumping: a protein relaxation following M formation results in a local rearrangement of the group, in the vicinity of the Schiff base. The rearrangement changes the accessibility of the Schiff base and provides that its deprotonation and reprotonation occur on different sides. The conformational change has characteristics typical for relaxations in proteins. In addition, it is shown that at 260 K an equilibrium exists between the M and N forms.

Light-driven proton transport by bacteriorhodopsin (bR) located in the purple membrane of *Halobacterium halobium* is extensively studied to understand the fundamental rules of energy transduction by proteins. bR is a protein–pigment complex: the chromophore is a retinal covalently bound to a lysine residue of the protein via a protonated Schiff base. Upon light absorption, light-adapted bR undergoes a series of transitions called the photocycle. It is approximately characterized by the reaction scheme (1):



The letters denote the successive intermediate states. During this photocycle, protons are transported from the inside of the cell to the extracellular medium. Photoelectric experiments show that proton pumping proceeds in several discrete steps simultaneously with the transitions of the cycle (2, 3). The proton transport occurs through protonable groups; aspartic and tyrosine residues have been shown to be members of the proton transport chain by Fourier transform infrared (FTIR) difference spectroscopy (4–9).

The changes of the retinal structure during the photocycle are fairly well understood from vibrational spectroscopic studies (10–13). After light absorption, the retinal undergoes an isomerization from all-trans to a distorted 13-cis configuration during the bR–K transition, the only light-driven

transition. In the subsequent K–L step, the retinal relaxes to the planar cis structure. In the L–M transition, the Schiff-base proton is released; the Schiff base is reprotonated in the M–N step. The crucial proton transport step is believed to occur at the transiently deprotonated Schiff base. The proton is first released towards the outside of the cell into a proton pathway in which the carboxylic group of the residue Asp-85 has been recently identified as a proton acceptor by FTIR difference spectroscopy (14) and photoelectric experiments (15) using site-directed mutant samples. In the M–N transition, the Schiff base is reprotonated from the opposite side through a proton pathway, a member of which is Asp-96 (14–18). In the N–O step, the cis–trans isomerization of the retinal occurs, and finally the protein relaxes to its initial state. According to this picture, proton release and uptake by Schiff base occur on different sides. However, the structure of the retinal does not change significantly between the L and N states (13). Therefore, Fodor *et al.* (13) postulated in their “T–C model” a crucial conformational switch: at or after the formation of M, a conformational change in the protein shifts the connectivity of the Schiff base. It is generally believed that protein conformational changes during the photocycle are important for proton pumping and have been demonstrated by a number of methods (11, 19–24). However, the molecular changes are not well determined, and their actual role in the process of proton transport is not known at all. Here I use FTIR difference spectroscopy to obtain more information about conformational changes during the photocycle and to elucidate their importance in proton transport.

METHODS

Sample Preparation. Purple membranes were isolated from *H. halobium* strain ET1001 as described by Oesterhelt and Stoekenius (25). Films of bR with an absorbance $A \approx 1$ at 570 nm were prepared by drying the purple membrane suspension on a Cleartran plate in vacuum. The samples were fully hydrated in a hygroscopic sample chamber for a day at room temperature. The pH and salt concentration of the sample are not well determined, but control flash photolysis experiments on these samples showed that the photocycle at room temperature is identical to that of bR in low salt concentration at about pH 6.

Experimental. Infrared spectra in the wavenumber range 700–2000 cm^{-1} were collected in a Mattson Sirius 100 FTIR spectrophotometer at a resolution of 2 cm^{-1} . The bR film was light-adapted at 300 K for 10 min with focused light from a 250-W tungsten lamp passing through a 15-cm pathlength water heat filter and a 530-nm glass high-pass filter. The same lamp and optics were used for subsequent illumination of the sample, but the color filters were varied. After light adaptation the sample was rapidly cooled to the desired tempera-

ture. A closed-circuit helium refrigerator (CTI model 21) controlled the temperature with accuracy and stability better than 0.2 K.

The slow-decay kinetics of the M form were followed. After the temperature had stabilized and a reference spectrum of bR_{LA} (LA refers to light-adapted) had been collected (an average of 250 scans), the photocycle was initiated by illuminating the sample through a 520-nm interference filter for 10 s (intensity = 8 mW/cm²). The sample spectrum collection was started immediately after illumination, and successive scans were performed. The number of scans was doubled for each successive spectrum. For the first spectrum, five scans were averaged. This resulted in an effective time resolution of about 15 s. The spectra then followed each other in a quasi-logarithmic time scale; therefore, the signal-to-noise ratio of the spectra improved with time. M - bR difference spectra were calculated by using the light-adapted bR reference spectrum, and the time evolution of the resulting difference spectra was later analyzed.

RESULTS AND DISCUSSION

The slow decay kinetics of the M form was followed in the temperature range from 240 K to 260 K. Based on previous experience, I expected a smooth temperature dependence of the M decay with similar spectral features. However, on raising the temperature, the observed transition changed its characteristics in addition to becoming faster. Fig. 1 shows the time dependence of the difference spectra $S(t) - S(t < 0)$. Illumination produces the typical difference spectrum characteristic of M (11, 26). To be able to discuss the M decay reaction in detail, I first summarize the spectral components upon which we shall focus our attention.

First, the negative band at 1526 cm⁻¹ represents the ethylenic vibration of the retinal in the bR state. It is negative because the M-bR mixture at time t contains less bR than the initial bR state at $t < 0$ —i.e., bR is "missing." The positive ethylenic band of M at 1564 cm⁻¹ is clearly seen in the spectra collected at 240 K. In the spectra at 260 K, this band is in the shoulder of the 1556 cm⁻¹ band that has been assigned as an amide II line having a large amplitude at higher temperatures (26).

Second, the positive band at 1624 cm⁻¹ and its negative counterpart at 1639 cm⁻¹ represent the Schiff-base vibration in the deprotonated and (missing) protonated states (11, 27), respectively. In our difference spectra, the total amplitude of this band pair is a measure of the Schiff-base deprotonation (it has been protonated in the bR state).

Third, the bands in the region 1760 cm⁻¹ to 1730 cm⁻¹ represent vibrations of protonated carboxylic groups of aspartic residues (5)—specifically, (i) the band at 1762 cm⁻¹ represents Asp-85, the primary proton acceptor (14) that is deprotonated in bR and protonated in M, and (ii) the negative band at 1742 cm⁻¹ represents Asp-96 (14, 16). There is some disagreement between refs. 14 and 16 concerning the protonation state that this band represents. Fortunately, these differences have no effect on my conclusions. It is only important that the band represents Asp-96 and that it is part of the Schiff-base reprotonation route from the cytoplasmic side.

Fourth, the amide I lines at 1669 cm⁻¹ and 1658 cm⁻¹ indicate protein conformational changes. The time evolution of the difference spectra at both 240 K (Fig. 1 Upper) and 260 K (Fig. 1 Lower) shows a slow decay of M toward the bR form, as indicated by the uniform disappearance of the ethylenic vibrations. If the data represented the decay of a single species into bR in a single step (as the change of the ethylenic vibrations suggests), all bands should decrease simultaneously. At both 240 K and 260 K, the M-to-bR transition (as defined by the ethylenic vibrations) proceeds

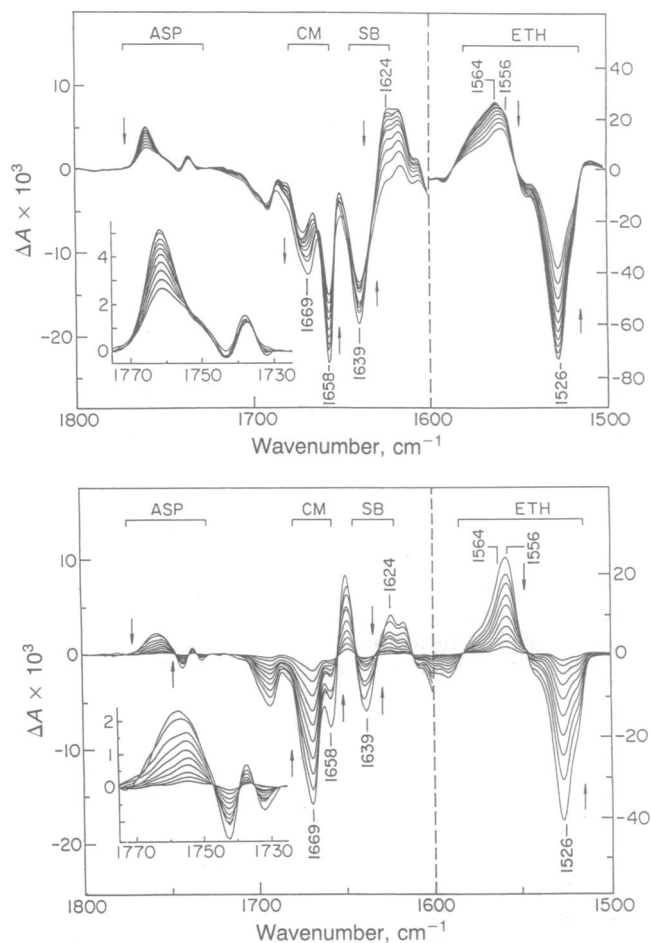


FIG. 1. Successive M - bR difference spectra (ΔA) following photolysis. The spectra follow each other in a quasi-logarithmic time scale; the first spectrum is taken at 15 s after photolysis and the last one at 50 min. Spectral regions: ASP, protonated carboxylic vibrations of aspartic residues; CM, conformational marker bands at 1669 cm⁻¹ and 1658 cm⁻¹; SB, Schiff-base vibration bands; ETH, ethylenic bands at 1526 cm⁻¹ and at 1564 cm⁻¹. Arrows indicate the direction of the time evolution of the bands. (Upper) Results at 240 K. (Lower) Results at 260 K. (Insets) Expanded protonated carboxylic carbonyl region.

simultaneously with the reprotonation of the Schiff base (characterized by the disappearance of the Schiff-base bands). However, the correlation of the spectral changes of other regions to this main process is very different at 240 K and 260 K.

(i) At 240 K the decay of the Asp-85 band coincides with the main process (the ethylenic and Schiff-base changes, Fig. 2), but no change is observed in the other bands in the aspartic spectral region, including the one representing Asp-96 (Fig. 1 Upper). The spectra show that reprotonation of the Schiff base occurs simultaneously with deprotonation of Asp-85, the only aspartic group to undergo change. We conclude that the Schiff base is reprotonated from Asp-85, the group to which the proton had been released during the L-M transition.

(ii) At 260 K the carboxylic band of Asp-85 has already disappeared by the time the first spectrum is taken, although again the slow decay of the ethylenic and Schiff-base reprotonation are observed. This observation means that the proton release from Asp-85 occurs fast and not to the Schiff base. The decay of the ethylenic vibrations and that of the Schiff base bands coincide in time with that of all other bands between 1757 cm⁻¹ and 1730 cm⁻¹, including the one at 1742 cm⁻¹ that represents Asp-96 (Fig. 1 Lower and Fig. 2). This

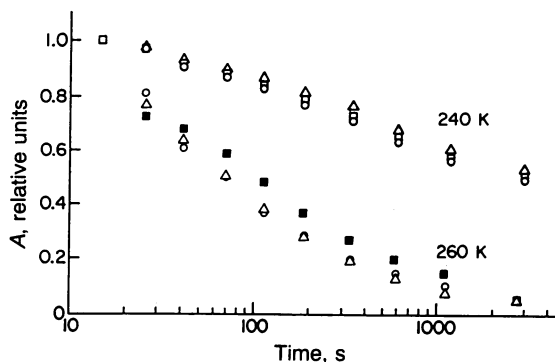


FIG. 2. Normalized amplitudes of characteristic bands from the data in Fig. 1 as a function of time. Δ , $A_{1526\text{cm}^{-1}}$ (amplitude of the bR ethylenic difference); \circ , $A_{1639\text{cm}^{-1}} + A_{1624\text{cm}^{-1}}$ (total amplitude of the Schiff-base differences); \square , $A_{1762\text{cm}^{-1}}$ (protonated Asp-85); \blacksquare , $A_{1742\text{cm}^{-1}}$ (the band representing Asp-96).

observation is expected if reprotonation of the Schiff base occurs through Asp-96 from the intracellular side. At both temperatures the shape of the retinal lines does not change with time, suggesting that M decays into bR in a single step at both 240 and 260 K. However, the reactions are very different.

In the reaction at 240 K, the aspartic lines between 1757 cm^{-1} and 1730 cm^{-1} do not change, and the amide I band at 1669 cm^{-1} even grows. Although the retinal changes are identical to those in a direct M-to-bR decay, the transition does not reach the bR form but indicates formation of a stable state that does not occur in the photocycle under physiological conditions.

In the reaction at 260 K the uniformly decaying spectrum is clearly characteristic of M, but it is distinctly different from those obtained at 240 K also in the retinal bands. Fig. 3 shows the first difference spectra obtained at 240 and 260 K in the fingerprint region, together with their normalized difference ($260\text{ K} - 240\text{ K}$) that was obtained by scaling to minimize the C—C single-bond bands of bR at 1167 cm^{-1} , 1202 cm^{-1} , and 1255 cm^{-1} . The subtraction results in a spectrum with a positive band at 1186 cm^{-1} . This band is seen as characteristic of N (13); therefore, the difference has to be assigned to N. I conclude that at 260 K, a mixture of M and N is seen. The positive band at 1397 cm^{-1} is most likely the carboxylate vibration of Asp-85 that was protonated in the early times at 240 K and is deprotonated at 260 K. In general, the similarity

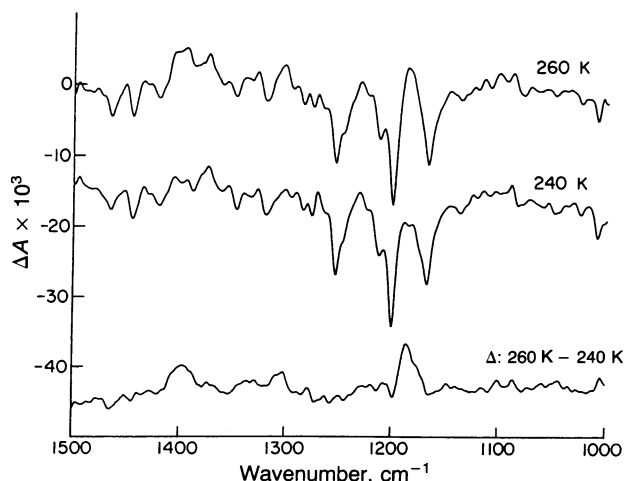


FIG. 3. Low wavenumber region of the M - bR difference spectra obtained 15 s after excitation at 240 K and 260 K, and their difference (Δ) after normalization to the C—C single bond vibration bands of bR (the spectrum of N).

of the spectrum of N and that of L (26) suggests a similar retinal structure in N and L, as also pointed out by Fodor *et al.* (13). During the decay the shape of the spectrum does not change significantly. This means that the M and N forms are in equilibrium, i.e., the kinetic equilibrium between M and N is faster than their decay at this temperature.

The dramatic change in the route of Schiff-base reprotonation between 240 K and 260 K is coupled to the exchange of the negative amide I bands at 1658 cm^{-1} and 1669 cm^{-1} , an additional striking difference between the spectra from 240 K and 260 K in Fig. 1 *Upper* and *Lower*. At 240 K the small-amplitude 1669-cm^{-1} band slowly grows (the only growing band), while at 260 K it is much larger than the band at 1658 cm^{-1} when the first spectrum is collected 15 s after excitation. The exchange of the two bands suggests a transition between two protein conformational states characterized by the ratio of the bands. To measure the extent of the conformational change, the relative extinction coefficients of the two conformational marker bands have to be known. They can be determined by normalizing the band amplitudes to the bR ethylenic band in the extreme cases where practically only one of the bands is present: $A_{1669\text{ cm}^{-1}}/A_{1658\text{ cm}^{-1}} = 1.6$ is found. If the two conformational states are represented by the bands at 1658 cm^{-1} and 1669 cm^{-1} , respectively, then the transition between the two states can be characterized by the following quantity:

$$r(t) = \frac{A_{1669\text{ cm}^{-1}}}{A_{1669\text{ cm}^{-1}} + 1.6A_{1658\text{ cm}^{-1}}} \quad [1]$$

However, at 260 K, after a couple of minutes $r(t)$ reaches a constant value of 0.92: a residual component of the 1658-cm^{-1} band remains in the spectrum after completion of the transition. Therefore, we define a transition parameter $\Phi(t) = r(t)/r(\infty)$ that changes between 0 and 1 to characterize the extent of the conformational transition. [This definition assumes that $r(0) = 0$ (i.e., in the initial state, only the 1658-cm^{-1} band is present). We have no data at $t = 0$; however, the smallest value of $r(t)$ measured is $r(t) = 0.03$. Therefore, the assumption, even if incorrect, cannot introduce significant errors.] $\Phi(t)$ is shown in Fig. 4.

At 240 K the reaction starts to take place very slowly on a time-scale different from the ethylenic and Schiff-base protonation changes. In roughly 1 hr it proceeds to about 20% completion (Fig. 4). At 260 K the conformational change $\Phi(t)$ is fast, and we only see the very end of the transition. In the protein state characterized by a large band at 1658 cm^{-1} and a small one at 1669 cm^{-1} [$\Phi(t) \ll 1$], Schiff-base reprotonation takes place from Asp-85. If, on the other hand, the protein transition takes place before Schiff-base reprotona-

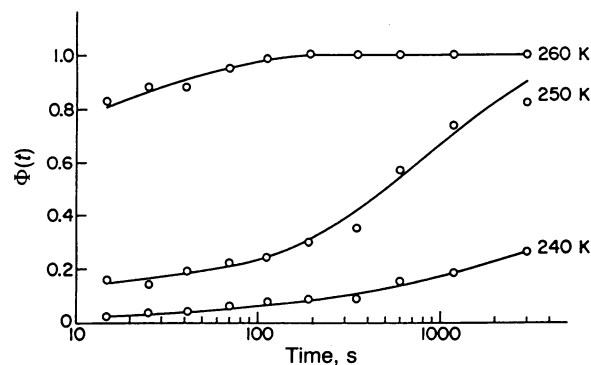


FIG. 4. Time (t) dependence of the protein relaxation parameter at different temperatures around 250 K. The lines are drawn to guide the eye.

tion, the normal pumping sequence is seen, and proton uptake occurs from the chain, a member of which is Asp-96.

Based on their kinetic behavior, two independent sets of reactions can be distinguished, both triggered by the formation of M: (i) the decay of the M form (or a mixture of M and N) as characterized by the ethylenic change and reprotonation of the Schiff base, and (ii) the protein conformational change characterized by $\Phi(t)$ (Fig. 4). The temperature dependence of their rates is very different: $\Phi(t)$ speeds up at least by a factor of 1000 between 240 K and 260 K, whereas the rate of the M decay only increases by a factor of about 10. Most remarkably, the relative rate of the two reaction sets (which is obviously also very sensitive to the temperature) determines the path of the reprotonation of the Schiff base. This also explains the slight apparent shift of the aspartic band in Fig. 1 Lower from 1758 cm^{-1} to 1754 cm^{-1} at 260 K at the early times: in the first spectrum a residual 1762-cm^{-1} component is present because of the incomplete protein transition.

The results can be explained in the framework of the T-C model for the proton-pumping mechanism (13), discussed in the introduction. We interpret the observed conformational change as the T-C conformational switch that changes the accessibility of the Schiff base necessary for proton pumping. The data suggest the following sequence of events in the normal pumping process (Fig. 5). During the L-to-M transi-

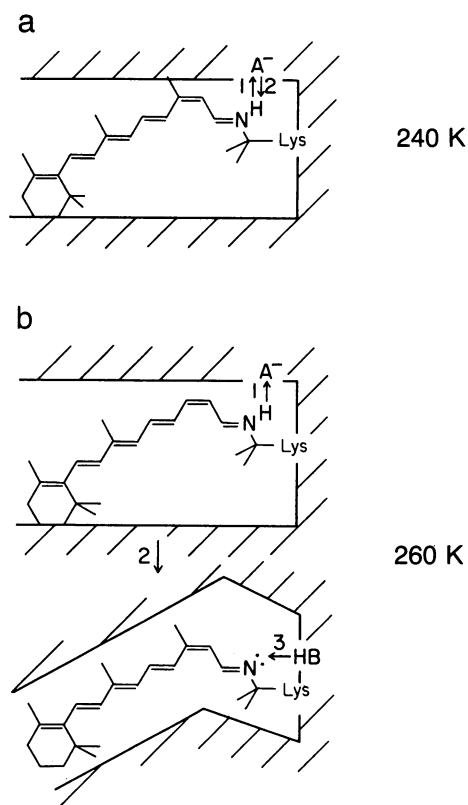


FIG. 5. The molecular events in bacteriorhodopsin associated with the M form. Representation analogous to the one introduced by Fodor *et al.* (13) is used. (a) Events at 240 K: Reaction 1 indicates M formation (L-M): Schiff-base deprotonation. Reaction 2 indicates M decay: Schiff-base reprotonation. The protein is frozen, the proton released to Asp-85 returns to the Schiff base, and no pumping occurs. (b) Events at 260 K. Reaction 1 indicates M formation (L-M): Schiff-base deprotonation. Reaction 2 indicates protein relaxation (T-C). Reaction 3 indicates M decay (M-N): Schiff-base reprotonation. Following deprotonation of the Schiff base, the T-C transition takes place (13), and Schiff-base reprotonation occurs from a donor (through Asp-96) in the proton-transport chain from the intracellular side.

tion, the Schiff base releases the proton to an acceptor into the proton-transport chain, a member of which is Asp-85. At the same time, the stress in the protein induced by the retinal with changed geometry triggers a protein conformational relaxation, which is observed as the change of the amide I lines at 1658 cm^{-1} and 1669 cm^{-1} . The relaxation results in a local rearrangement of groups in the vicinity of the Schiff base, thereby changing its accessibility. Reprotonation then occurs from a donor group at the end of the proton transport chain from the cytoplasmic side of the membrane, a member of which is Asp-96. At physiological temperatures, the C-T transition is predicted to be very fast—not observable with our technique. At low temperatures (in this case 240 K) where the protein is “frozen,” even though the retinal has assumed the shape and protonation state characteristic for the M form, the protein is not able to readjust the shape to relieve the stress (assume the C form), and the proton is picked up from where it has been released: there is no pumping. As already discussed, in this case the decay of M results in a non-physiological state. The N intermediate can only be formed if the T-C transition precedes Schiff-base reprotonation. The experiment is a verification of the T-C conformational-switch model (13) as opposed to earlier suggestions where conformational change of only the retinal was supposed to provide the proper directionality of the deprotonation and subsequent reprotonation steps of the Schiff base (28). This crucial conformational change is well characterized by the ratio of the amide I bands at 1658 cm^{-1} and 1669 cm^{-1} . At this point it is not possible to connect it directly to specific structural features. Nevertheless, the transition suggests changes in hydrogen bonding of the amide C=O bonds (this typically causes a shift of the carbonyl frequencies of such size). There are additional differences between the difference spectra: (i) in the spectra taken at 240 K (Fig. 1 Upper), a broad negative band is seen in the amide I region, and (ii) the relative amplitude of the amide II line at 1556 cm^{-1} is much larger at 260 K (Fig. 1) as previously reported and interpreted as a marker of a conformational change (26). These differences also suggest connection to the conformational transition reported here. It has to be emphasized, however, that the T-C conformational switch, although crucial, probably is not the only one during the whole photocycle. The successive steps of the pumping process most likely involve several important transitions of the protein; their characterization is needed for the full understanding of the function.

The results demonstrate the importance of the protein in the pumping process; it is not merely a structural unit that provides the site for the retinal and a path for the protons across the membrane. The protein is an active participant in the process, and the features of the action fully support the general picture about the function of proteins introduced by Ansari *et al.* (29). According to this model the crucial conformational changes [functionally important motions (FIMs)] in the proteins are triggered by a stress induced by a deformation of the prosthetic group. The strain energy is dissipated through the propagation of a deformation (protein quake). These relaxations (FIMs) are nonequilibrium transitions between states of a fluctuating protein. If the molecule is frozen, the protein transitions do not occur. The process of energy transduction involves successive conformational changes of the chromophore and the apoprotein; transitions of both are crucial for the proper function, and the critical sequence of these relaxations is determined by the design of the protein.

The kinetics and temperature dependence of the described protein relaxation point to another general feature of proteins. The large temperature dependence of the nonexponential rate (over a factor of 1000 at a temperature increase of 20 K) (Fig. 5) indicates non-Arrhenius behavior. Similar kinetic properties and comparable temperature dependence are

found in relaxations induced by pressure jump in myoglobin in glycerol/water solvent around 200 K (30). Detailed investigation there showed that they can be described by parameters characteristic of relaxations in glasses. The data presented here then also show the glassy behavior of proteins; glass transitions are vital for the function. It is important to note that the transition occurs around 250 K. This temperature region is believed to be the melting temperature of bound water in proteins (31): the protein together with the molten bound water is the functioning protein. The importance of water in the proton pumping was demonstrated by photoelectric experiments (32). Also, the protein conformational change seen by the increase of the 1556-cm^{-1} amide II band was seen to take place only in the presence of water (26).

In the discussion of my results, the simplest model of the photocycle (1) is used. The nature of my experiments and data is not suited for detailed kinetic analysis of more complicated specific schemes. The observed phenomena are obviously compatible with several kinetic models. However, the results have important consequence of general value concerning possible kinetic schemes. The photocycle is not a simple chain of consecutive reactions with comparable activation parameters. Events during the photocycle trigger independent reactions with very different thermal characteristics, and the relative rates of the different processes may result in different states. Therefore, the whole pattern of reactions may change by changing the temperature [such as temperature-dependent branching from L to bR or from M to bR, etc. (e.g. ref. 33)].

In the present case, I observed that even the M-to-bR decay completely changes its character between 240 K and 260 K. I have shown that at 240 K the apparent M-to-bR transition actually results in a state in which the protein is different from that in the bR state; the product is in a nonphysiological form. Consequently, prediction of events based on extrapolation to very different temperatures is not straightforward at all, and it has to be verified in each case.

I thank H. Frauenfelder, L. Keszthelyi, M. S. Braiman, T. G. Ebrey, W. Stoeckenius, P. G. Wolynes, R. D. Young, G. U. Nienhaus, and A. Xie for constructive remarks and many stimulating discussions. This work was supported by National Institutes of Health Grant GM 32455.

1. Lozier, R. H., Bogomolni, R. A. & Stoeckenius, W. (1975) *Biophys. J.* **15**, 955–962.
2. Drachev, L., Kaulen, A. D. & Skulachev, V. P. (1978) *FEBS Lett.* **87**, 161–167.
3. Keszthelyi, L. & Ormos, P. (1980) *FEBS Lett.* **109**, 189–193.
4. Siebert, F. & Mantele, W. (1982) *FEBS Lett.* **141**, 82–87.
5. Engelhard, M., Gerwert, K., Hess, B., Kreutz, W. & Siebert, F. (1985) *Biochemistry* **24**, 400–407.
6. Rothschild, K. J., Roepe, P., Ahl, P. L., Earnest, T. N., Bogomolni, R. A., Das Gupta, S. K., Mulliken, C. M. & Herzfeld, J. (1986) *Proc. Natl. Acad. Sci. USA* **83**, 347–351.
7. Dollinger, G., Eisenstein, L., Lin, S.-L., Nakanishi, K. & Termini, J. (1986) *Biochemistry* **25**, 6524–6533.
8. Dollinger, G., Eisenstein, L., Lin, S.-L., Nakanishi, K., Odashima, K. & Termini, J. (1986) *Methods Enzymol.* **127**, 649–662.
9. Lin, S.-L., Ormos, P., Eisenstein, L., Govindjee, R., Konno, K. & Nakanishi, K. (1987) *Biochemistry* **26**, 8327–8331.
10. Braiman, M. S. & Mathies, R. A. (1982) *Proc. Natl. Acad. Sci. USA* **79**, 403–407.
11. Bagley, K., Dollinger, G., Eisenstein, L., Singh, A. K. & Zimanyi, L. (1982) *Proc. Natl. Acad. Sci. USA* **79**, 4972–4976.
12. Smith, S. O., Lugtenburg, J. & Mathies, R. A. (1985) *J. Membr. Biol.* **85**, 95–109.
13. Fodor, S. P. A., Ames, J. B., Gebhard, R., van den Berg, E. M. M., Stoeckenius, W., Lugtenburg, J. & Mathies, R. A. (1988) *Biochemistry* **27**, 7097–7101.
14. Braiman, M. S., Mogi, T., Marti, T., Stern, L. J., Khorana, H. G. & Rothschild, K. J. (1988) *Biochemistry* **27**, 8516–8520.
15. Butt, H. J., Fendler, K., Bamberg, E., Tittor, J. & Oesterhelt, D. (1989) *EMBO J.* **8**, 1657–1663.
16. Gerwert, K., Hess, B., Soppa, J. & Oesterhelt, D. (1989) *Proc. Natl. Acad. Sci. USA* **86**, 4943–4947.
17. Otto, H., Marti, T., Holz, M., Mogi, T., Lindau, M., Khorana, H. G. & Heyn, M. P. (1989) *Proc. Natl. Acad. Sci. USA* **86**, 9228–9232.
18. Tittor, J., Soell, Ch., Oesterhelt, D., Butt, H.-J. & Bamberg, E. (1989) *EMBO J.* **8**, 3477–3482.
19. Rothschild, K. J., Zagaeski, M. & Cantore, W. A. (1981) *Biochem. Biophys. Res. Commun.* **103**, 483–489.
20. Beece, D., Bowne, S., Czege, J., Eisenstein, L., Frauenfelder, H., Good, D., Marden, M. C., Marque, J., Ormos, P., Reinisch, L. & Yue, K. T. (1981) *Photochem. Photobiol.* **33**, 517–521.
21. Czege, J. (1988) *FEBS Lett.* **242**, 89–92.
22. Dencher, N. A., Dresselhaus, D., Zaccai, G. & Büldt, G. (1989) *Proc. Natl. Acad. Sci. USA* **86**, 7876–7879.
23. Rothschild, K. J., He, Y. W., Gray, D., Roepe, P. D., Pelltier, S. L., Brown, R. S. & Herzfeld, J. (1989) *Proc. Natl. Acad. Sci. USA* **86**, 9832–9835.
24. Gerwert, K., Hess, B. & Engelhard, M. (1990) *FEBS Lett.* **261**, 449–454.
25. Oesterhelt, D. & Stoeckenius, W. (1974) *Methods Enzymol.* **31**, 667–681.
26. Braiman, M. S., Ahl, P. L. & Rothschild, K. J. (1987) *Proc. Natl. Acad. Sci. USA* **84**, 5221–5225.
27. Gerwert, K. & Siebert, F. (1986) *EMBO J.* **5**, 805–811.
28. Schulten, K. & Tavan, P. (1978) *Nature (London)* **272**, 85–86.
29. Ansari, A., Berendzen, J., Bowne, S. F., Frauenfelder, H., Iben, I. E. T., Sauke, T. B., Shyamsunder, E. & Young, R. D. (1985) *Proc. Natl. Acad. Sci. USA* **82**, 5000–5004.
30. Iben, I. E. T., Braunstein, D., Doster, W., Frauenfelder, H., Hong, M.-K., Johnson, B. J., Luck, S., Ormos, P., Schulte, A., Steinbach, P., Xie, A. H. & Young, R. D. (1988) *Phys. Rev. Lett.* **62**, 1916–1920.
31. Parak, F. (1986) *Methods Enzymol.* **127**, 196–206.
32. Varo, Gy. & Keszthelyi, L. (1983) *Biophys. J.* **43**, 47–51.
33. Kalisky, O. & Ottolenghi, M. (1982) *Photochem. Photobiol.* **35**, 109–115.